

PAPER • OPEN ACCESS

Stress analysis of multi-layered composite cylinders subjected to various loadings

To cite this article: M H Elgohary *et al* 2021 *IOP Conf. Ser.: Mater. Sci. Eng.* **1172** 012005

View the [article online](#) for updates and enhancements.



ECS **240th ECS Meeting**
Digital Meeting, Oct 10-14, 2021
We are going fully digital!
Attendees register for free!
REGISTER NOW

Stress analysis of multi-layered composite cylinders subjected to various loadings.

M H Elgohary¹, M I El-Geuchy², H M Abdallah¹ and S S Sayed¹

¹ Rockets Department, Military Technical College, Cairo, Egypt

² PhD., Technical Research Centre, Cairo, Egypt

E-mail: Gohary1@live.com

Abstract: Composite cylinders are widely used in many applications, common examples for these applications are power drive shafts, chemical storage tanks, rocket motor cases and pressure vessels used in aerospace vehicles. The structure of the composite cylinder can be represented as a cylinder composed of coaxial orthotropic layers. In this paper, an analytical method is used to calculate stresses, strains and displacements through the wall thickness of multi-layered composite cylinder made of orthotropic material. The method is based on the theory of elasticity of bodies having cylindrical anisotropy. This method permits accurate stress analysis of thin and thick-walled composite cylinders subjected to axial load, torsional load and bending moment. The analytical method is modified to incorporate internal and external pressure loads beside the prescribed load cases. A numerical example is presented for a composite cylinder subjected to internal pressure load with a tensile axial load. The resulted stresses and strains are used to validate 3-dimensional finite element model. A parametric study has been performed using the analytical method to investigate the influencing parameters on stress distribution within the cylinder thickness and the results are found to be beneficial to look into during the preliminary design phase.

1. Introduction

Composite cylinders or pipes are laminated structures used in many applications such as pressurized fluid transportation or rocket motors manufactured using filament winding technology. With many advantages over conventional material, laminated composite cylinders are increasingly utilized due to their better stiffness to weight, strength to weight ratios and specific properties as corrosion resistance and chemical stability.

The first stumble for this type of industry and material is the many parameters involving the final design of the product. Due to design complexity parameters of interactions, trial and error in testing or manufacturing the composite products is very expensive and time consuming. Hence, there must be a method to decrease the number of experimentations to reach the final design, like implementing a mathematical model to perform a parametric study and finding out the effective parameters that control the design.

Mathematical analysis of laminated composite structures is used to predict their mechanical behavior using many approaches; one of the effective approaches is Lekhnitskii's approach [1], which used the three-dimensional theory of anisotropic elasticity to predict stresses and strains inside the thickness of composite laminates with fairly good accuracy.



Panda and Natarajan [2],[3] performed a finite element analysis technique on laminated composite plates and shells to predict the stresses within the laminates of the structure and compared their findings with elasticity and exact solution finding high accuracy between their work and exact solution with thickness to radius ratio of (20.5) which was used in their example. Finite element analysis is very important as it is able to deal with more complex shapes and details than the analytical methods, also it is able to get slightly more accurate results when compared with same case conditions. The hindrance of such technique is the requirement of high computing devices and the large time of setting the conditions; for which the preliminary analysis and design of products require too much parameters changes until reaching a semifinal design. For example, the analysis of plies in finite element requires at least one element per ply in case of composite laminates to get acceptable outcomes and since the composite ply is usually less than 1 mm the meshing of such model would require large solving time while in theoretical analysis once the equation parameters are calculated, the parameters change and corresponding stress and strains calculations would just require a fraction of the time needed in finite element.

Joulicoeur and Cardou [4] derived the stress functions to calculate stress distribution within the cylinder thickness. They used Lekhnitskii's approach to solve a system of two coaxial hollow circular cylinders under bending, torsion and tensile loads. They found that there is no coupling between bending and tension-torsion loads, also the curvature caused by the bending load is in a plane that is perpendicular to the moment axis. Wild and Vickers [5] used Lekhnitskii's approach to predict stress distribution along the thickness including a combined loading of centrifugal, axial, and pressure loads. Bakaiyan et al. [6] also used the three-dimensional elasticity theory to inspect composite pipes under thermomechanical loads showing that hoop to axial stresses or strains tends increasing while increasing the winding angle and the opposite when decreasing the angle to axial direction. Sun et al. [7] who presented an analysis strategy to analyze stresses for composite cylindrical structures which resulted in finding that material anisotropy has great effect on the coupling stiffness coefficients for axial and torsional loads while having almost no effect on the bending stiffness coefficients as bending load is uncoupled with other load types.

Menshykova and Guz [8] made a comparative study on the stress analysis of composite cylinders under bending load and how the stress variation within the thickness of the composite cylinders is affected by the material and winding angle of the composite plies.

Pham et. al. [9] studied the usage of composite material in the oil transportation by composite tubes and their advantages to using conventional material in weight saving and how composites may have design and manufacturing complications according to their application. Guz et. al. [10] also studied different materials for long fiber reinforced filament wound composite cylinder under different loadings.

Mohanavel et. al. [11] modeled an aluminum matrix composite (AMC) pressure vessel using FEA to investigate the extreme usage of the material to estimate the life usage of the material to increase its service time.

Sharma et. al. [12] performed a theoretical analysis using ANSYS to simulate a 35 MPa hydrogen pressure vessel and verified the results experimentally within 10% error. A weight reduction has been achieved by changing the winding pattern design basis by at least 15%.

Moshir et. al. [13] discussed the behavior of composite thick tubes using 3D elasticity theory and compared it to different analysis methods to determine the stiffness and strains in the tube subjected to bending load. They concluded that while FEA can be accurate and its results agree with the experimental data, the 3D elasticity solution can be simpler and less time consuming.

The method used in this paper is an analytical method comparable with previous work by other authors[7],[14],[6]. The analytical solution used was derived by Joulicoeur and Cardou was used and extended to incorporate the static pressure loads on the internal surface of the inner cylinder and external surface of the outer cylinder beside axial load, torsion, and bending loading applied on a multi-layered composite cylinder. The work will be presented in the following section with validation by previous work and comparison to finite element model using the commercial software ANSYS ACP module.

2. Theoretical work

2.1. Objective and problem description

This study targets the derivation of a mathematical model of the laminated composite cylinder to produce a system of equations able to predict the stresses and strains within the cylinder thickness in a combined cylinder loaded under internal pressure, torsion, axial load and bending. The system at study is a combination of any number of concentric cylinders, figure 1. Each of them has an internal and external radius. The internal first cylinder is hollow and its external radius is the second cylinder's internal radius and so on. Figure 1.2 shows an example of a combined cylinder consists of n -concentric cylinders; each of different helix angle α_i , where i is the number of cylinders composing the composite cylinder.

As shown in figure 2.1 the combined cylinder is subjected to axisymmetric loadings; axial load (P), torsion (C), internal and external pressure (P_{int} , P_{ext}) on surfaces (a) and (b) respectively denoted by the radii in figure 2.2. The cylinder could also be subjected to pure bending loads (M_x , M_y) in combination with the axisymmetric load. The resulting deformations due to these loads are global axial strain (ϵ), rotation per unit length (θ) and curvatures of the center line about the x and y axes (κ_x , κ_y). The combined cylinder has cylindrical anisotropy about the z axis. The coordinate system used here will be the cylindrical one, with cylinder axis (z) and (r , θ) as radial and tangential axes. All of the resultant stress and strains are functions of these coordinates only.

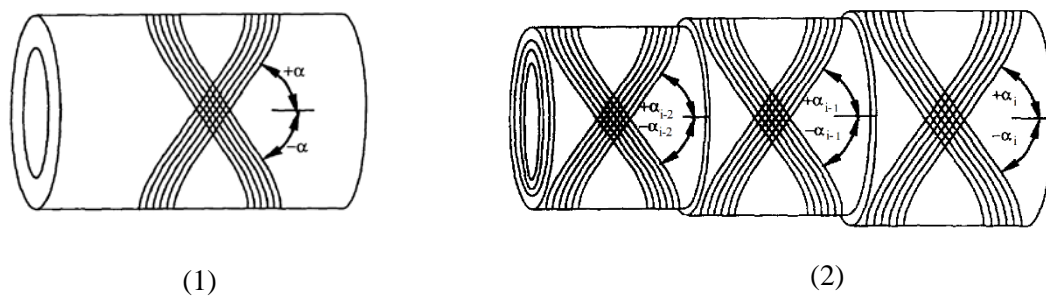


Figure 1. Scheme of composited laminated cylinder manufactured using filament winding

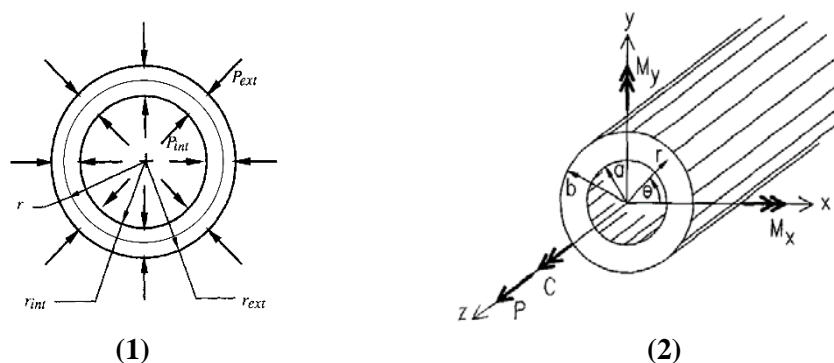


Figure 2. (1) Example of combined composite cylinder
(2) Loads and dimensions on the combined cylinder

The used material has orthotropic properties in which are defined by the fiber axis and the perpendicular directions, one in the same plane of the cylindrical ply (plane θ - z) and the other in the radial direction. The following assumptions are used in the analysis: the applied loads are constant along the z -axis, the body deformations are considered to be infinitesimal and elastic, resultant shear loads

equal to zero, the resultant stresses and strains are independent of the z-axis, meaning that the curvature due to bending is constant.

2.2. Fundamental equations

Each cylinder has nine elastic independent constants in three principle directions (1, 2, 3) of its orthotropic material in its local coordinate system which has the fibre axis as the first axis of the material coordinate system. It is assumed that these constants are known from the material properties from mechanical testing or datasheet of the material. With these constants known, they are transformed into the compliance matrix for the global coordinate system of the composite cylinder. This transformation is done on the radial axis by the complement of the helix angle.

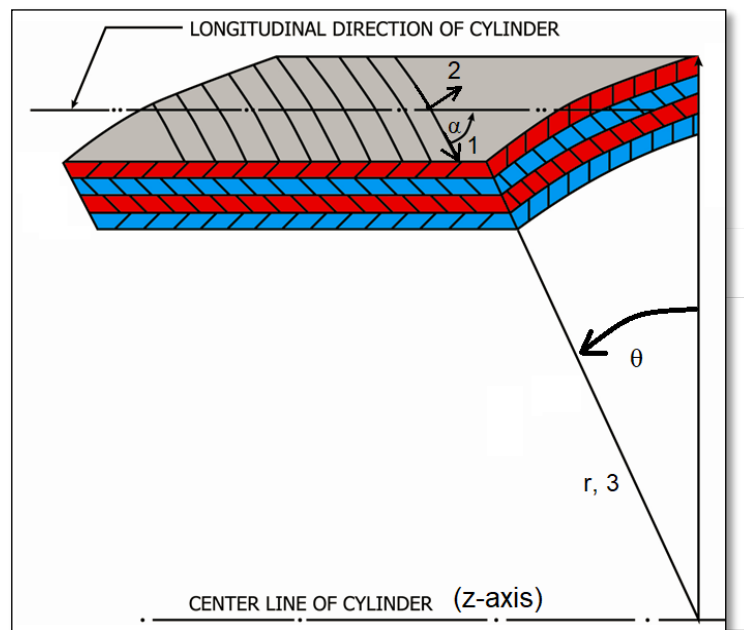


Figure 3. Coordinate Systems for composite material and cylinder

The transformed compliance matrix $[\check{S}]$ is calculated by:

$$[\check{S}] = [T]^{-1}[S][T] \quad (1)$$

The matrix $[C]$ is used to calculate the reduced elastic constants $[\beta]$ defined by Lekhnitskii by

$$\beta_{ij} = C_{ij} - \frac{C_{i3}C_{3j}}{C_{33}} \quad (2)$$

Noting that $\beta_{i3} = \beta_{3j} = 0$

2.3. Stress Functions

The stress components can be expressed using two functions $F(r, \theta)$ and $\Psi(r, \theta)$ derived by Lekhnitskii [1] using a system of partial differential equations that represent our problem. They are defined by

$$\sigma_r = \frac{\partial F}{r \partial r} + \frac{\partial^2 F}{r^2 \partial \theta^2}$$

$$\sigma_\theta = \frac{\partial^2 F}{\partial r^2}$$

$$\tau_{r\theta} = \frac{\partial F}{r^2 \partial \theta} - \frac{\partial^2 F}{r \partial r \partial \theta} \quad (4)$$

$$\tau_{rz} = \frac{\partial \Psi}{r \partial \theta} \quad (5)$$

$$\tau_{\theta z} = -\frac{\partial \Psi}{\partial r} \quad (6)$$

2.4. Separation of variables

To obtain a system of ordinary differential equations, Joulicoeur and Cardou [4] used separation of variables to acquire a solution in the form of

$$F = f_1(r)(\kappa_x \sin \theta - \kappa_y \cos \theta) + f_2(r) \quad (8)$$

$$\Psi = \psi_1(r)(\kappa_x \sin \theta - \kappa_y \cos \theta) + \psi_2(r) \quad (9)$$

the solution is divided into two systems, the first system in terms of f_1 and ψ_1 representing pure bending problem and the second system in terms of f_2 and ψ_2 representing axisymmetric problem.

2.4.1. Solution of Pure Bending system

The system mentioned is of the Cauchy-Euler type. This homogenous system is solved using the form

$$f_1 = Kr^{m+1} \quad (10);$$

$$\psi_1 = Kgr^m \quad (11)$$

Where K is an arbitrary constant

2.4.2. Solution of axisymmetric system

Lekhnitskii solved the general system as follows:

$$f_2 = \sum_{i=1}^2 \frac{K'_i}{m'_i + 1} r^{m'_i+1} + K'_3 + K'_4 r + \frac{K'_5}{2} r^2 + \frac{\mu_3}{3} \vartheta r^3 \quad (12)$$

$$\psi_2 = \sum_{i=1}^2 \frac{K'_i g'_i}{m'_i} r^{m'_i} + K'_4 \frac{\beta_{11}}{\beta_{14}} \ln r + K'_5 \frac{\beta_{14} + \beta_{24}}{\beta_{44}} r + K'_6 + \frac{C_{34}}{C_{33} \beta_{44}} \varepsilon r + \frac{\mu_4}{2} \vartheta r^2 \quad (13)$$

Where K'_i are six arbitrary constants

2.5. General complete solution

The complete general solution written using the previous results would be as follows:

$$F = (\kappa_x \sin \theta - \kappa_y \cos \theta) \left(\sum_{i=1}^4 \frac{K_i}{m_i} r^{m_i+1} + K_5 r + K_6 r \ln r + \frac{\mu_1}{2} r^3 \right) + \sum_{i=1}^2 \frac{K'_i}{m'_i + 1} r^{m'_i+1} + K'_3 + K'_4 r + \frac{K'_5}{2} r^2 + \frac{\mu_3}{3} \vartheta r^3 \quad (14)$$

$$\Psi = (\kappa_x \sin \theta - \kappa_y \cos \theta) \left(\sum_{i=1}^4 K_i g_i r^{m_i} + K_6 \frac{\beta_{56}}{\beta_{66}} + \mu_2 r^2 \right) + \sum_{i=1}^2 \frac{K'_i g'_i}{m'_i} r^{m'_i} + K'_4 \frac{\beta_{11}}{\beta_{14}} \ln r + K'_5 \frac{\beta_{14} + \beta_{24}}{\beta_{44}} r + K'_6 + \frac{C_{34}}{C_{33} \beta_{44}} \varepsilon r + \frac{\mu_4}{2} \vartheta r^2 \quad (15)$$

2.6. Stresses and strains equations

$$\sigma_r = (\kappa_x \sin \theta - \kappa_y \cos \theta) \left(\sum_{i=1}^4 K_i r^{m_i-1} + \mu_1 r \right) + \sum_{i=1}^2 K'_i r^{m'_i-1} + \mu_3 \vartheta r + \mu_5 \varepsilon \quad (16)$$

$$\sigma_\theta = (\kappa_x \sin \theta - \kappa_y \cos \theta) \left(\sum_{i=1}^4 K_i (m_i + 1) r^{m_i-1} + 3\mu_1 r \right) + \sum_{i=1}^2 K'_i m'_i r^{m'_i-1} + \mu_3 \vartheta r + \mu_5 \varepsilon \quad (17)$$

$$\tau_{r\theta} = (\kappa_x \cos \theta + \kappa_y \sin \theta) \left(- \sum_{i=1}^4 K_i r^{m_i-1} - \mu_1 r \right) \quad (18)$$

$$\tau_{rz} = (\kappa_x \cos \theta + \kappa_y \sin \theta) \left(\sum_{i=1}^4 K_i g_i r^{m_i-1} + \mu_2 r \right) \quad (19)$$

$$\tau_{\theta z} = (\kappa_x \sin \theta - \kappa_y \cos \theta) \left(- \sum_{i=1}^4 K_i g_i m_i r^{m_i-1} - 2\mu_2 r \right) - \sum_{i=1}^2 K'_i g'_i r^{m'_i-1} - \mu_4 \vartheta r - \left(\mu_5 \frac{\beta_{14} + \beta_{24}}{\beta_{44}} + \frac{C_{34}}{C_{33}\beta_{44}} \right) \varepsilon \quad (20)$$

$$\sigma_z = \frac{1}{C_{33}} [\kappa_x r \sin \theta - \kappa_y r \cos \theta + \varepsilon - C_{13}\sigma_r - C_{23}\sigma_\theta - C_{34}\tau_{\theta z}] \quad (21)$$

2.7. Boundary conditions

To obtain the unknown constants K_i , K'_i and global deformations ε , ϑ , κ one should study the boundary conditions of case. Rigid-body displacements are also considered to maintain displacement compatibility of several coaxial cylinders; and it was found that assuming the rigid body displacement are equal to zero would overdetermine the problem in hand although its customary in this type to assume some of these displacements to be equal to zero.

From this point, the modification of the method is presented by adding the internal and external pressure in the boundary conditions to incorporate them in the solution. This will affect the part of axisymmetric loading case as shown in the next section. The theory could be used for cylinders that are bonded together or just coaxial cylinders with no friction between them maintaining no loss of contact between them. The concerned case is for the cylinders that are perfectly bonded together.

2.8. End conditions

$$P = \sum_{n=0}^N \int_0^{2\pi} \int_{r_a}^{r_b} \sigma_z r \, d\theta \, dr \quad (22)$$

$$C = \sum_{n=0}^N \int_0^{2\pi} \int_{r_a}^{r_b} \tau_{\theta z} r^2 \, d\theta \, dr \quad (23)$$

$$M_x = \sum_{n=0}^N \int_0^{2\pi} \int_{r_a}^{r_b} \sigma_z r^2 \sin \theta \, d\theta \, dr \quad (24)$$

$$M_y = - \sum_{n=0}^N \int_0^{2\pi} \int_{r_a}^{r_b} \sigma_z r^2 \cos \theta d\theta dr \quad (25)$$

Such that P, C, M_x, M_y are external forces and moments.

Leading eventually to:

$$\begin{Bmatrix} \varepsilon \\ \vartheta \end{Bmatrix} = A \begin{Bmatrix} P_a \\ P_b \end{Bmatrix} + B \begin{Bmatrix} P \\ C \end{Bmatrix} \quad (26)$$

Where

$$A = (M3[M1]^{-1}[M2] + M4)^{-1} M3[M1]^{-1} (-M_p) \quad (27)$$

$$B = (M3[M1]^{-1}[M2] + M4)^{-1} \quad (28)$$

And P_a, P_b are the internal and external pressures of the inner and outer surfaces of the combined cylinder.

3. Case study with numerical examples

To get a clear comparison of results, all materials used in mathematical and finite element models are mentioned in the following table.

Table 1. Mechanical properties of the used composite materials in the study

	E ₁ (GPa)	E ₂ (GPa)	E ₃ (GPa)	ν ₂₃	ν ₁₃	ν ₁₂	G ₂₃ (GPa)	G ₁₃ (GPa)	G ₁₂ (GPa)
Graphite-polymer composite [15]	155	12.1	12.1	0.458	0.248	0.248	3.2	4.4	4.4
T300/934 [14]	141.6	10.7	10.7	0.495	0.268	0.268	3.88	3.88	3.58
Glass Reinforced Epoxy [15]	50	15.2	15.2	0.428	0.254	0.254	3.28	4.7	4.7
Kevlar49/Epoxy[16]	75	6	6	0.34	0.34	0.34	2	2	2

Table 2. Mechanical strength of the used composite materials in the study

	S ₁ ^T (MPa)	S ₂ ^T (MPa)	S ₃ ^T (MPa)	S ₁ ^C (MPa)	S ₂ ^C (MPa)	S ₃ ^C (MPa)	τ ₆ (MPa)	τ ₄ (MPa)	τ ₅ (MPa)
Graphite-polymer composite [15]	1500	50	50	1250	200	200	100	30	30
T300/934 [14]	2280	57	57	1725	228	228	76	60	76
E-Glass Epoxy [17]	1140	39	39	620	128	128	89	44	41

An implemented code ran by MATLAB using one or more of the materials mentioned in table 1 of four concentric cylinders each of 0.5 mm thickness with the composite cylinder inner radius of 50 mm under internal pressure of 10 MPa with closed ends (combined biaxial loads) is used to simulate stresses and strains with wall thickness of the cylinder.

4. Finite element analysis

Using ANSYS workbench and ACP module, a replica of the numerical case study example is done to compare results. The model used a custom material with the same mechanical properties used in the numerical example and in table 1. The finite element model shown in figure 5 shows a stress variation

along the z-axis of the cylinder despite the numerical example assumption and this is due to the boundary conditions placed on the edges of the cylinder; one for the support and one for the axial force. And to overcome this variation the results are taken exactly at the middle of the cylinder within the thickness of the cylinder by making a construction path in the finite element model and comparing the results with the analytical model.

Starting with a shell 2D model then using the ACP module to create the solid model with the prescribed material plies thickness and orientation; meshed with a 3D solid element (8 noded Hexahedron type Hex8) shown in figure 4 with nodal solution and maximum element size of 2 mm which is the thickness of one ply. SOLID185 Element which is used for 3-D modeling of solid structures is used as in this simulation. Defined by eight nodes the element has three degrees of freedom at each node: translations in the nodal x, y, and z directions, with large strain capabilities and other mechanical properties as hyper elasticity and plasticity.

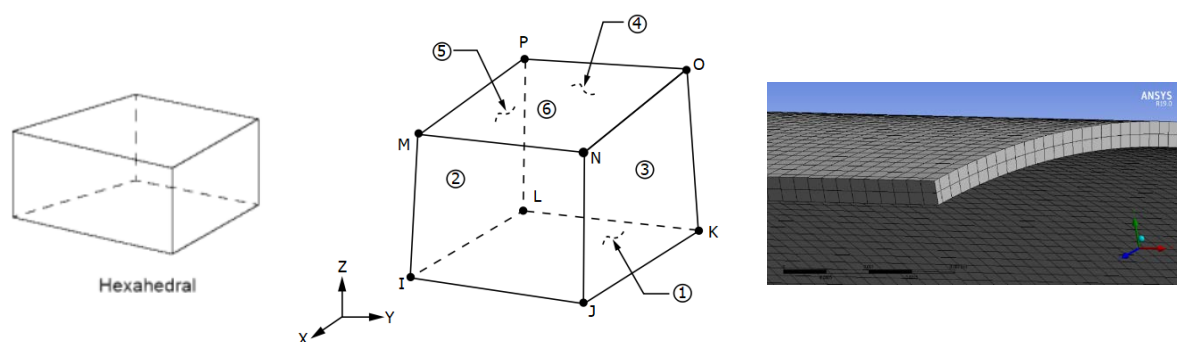


Figure 4. Solid model element used in the analysis (SOLID185 - 3-D 8-Node Structural Solid)

The mesh size element is chosen at least equal to one ply thickness as shown in figure 6. This was found in agreement with ref [7] as if the element size has increased more than one ply thickness, the output results would have a much increased error margin and low accuracy. And using less element size would require much more computational power with slight increase in output results accuracy.

To check the reliability of the finite element model agreement with the analytical model, the above-mentioned cylinder geometry has been checked with two of the most common used winding angles ($\pm 55^\circ$, $\pm 30^\circ$) with different stacking sequences. The analytical model assumes constant stresses and strains through the axial direction while the finite element maybe affected by the boundary conditions necessary for the software calculations. The results of the finite element modeling show an agreement with the analytical results as shown in figure 7. By comparing the output results the error margin stays at less than 5% difference between the analytical model and the finite element model which is quite good. It's worth mentioning that the model implemented by the finite element software needs much more time to program into the software and each case would take quite the time to give results and take these results into other platform to compare; which is all fine and even versatile and accurate for

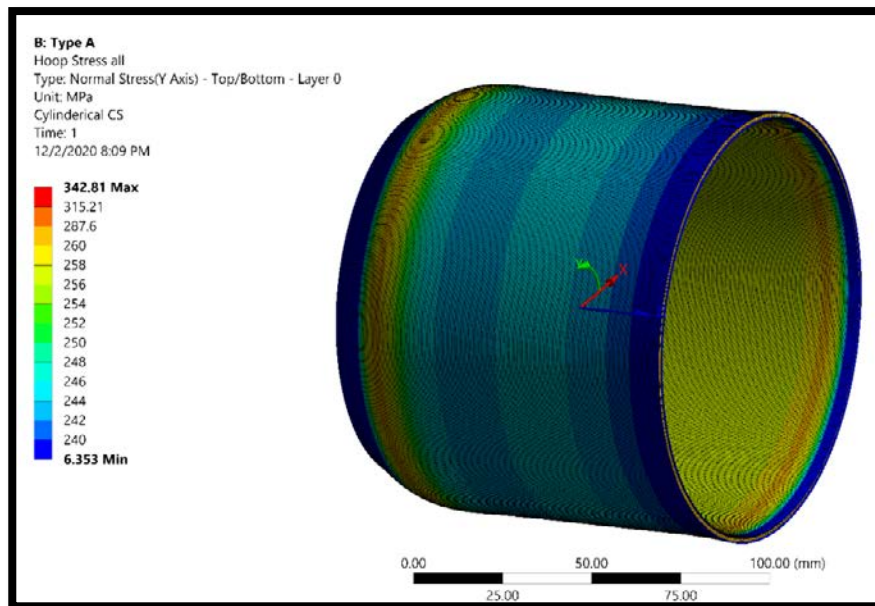


Figure 5. Hoop stresses on the numerical model

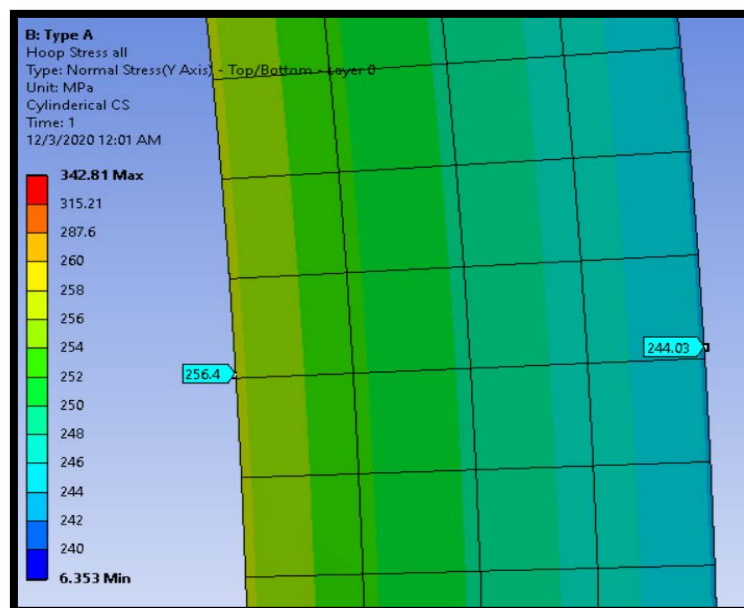


Figure 6. Numerical model elements within the thickness of the cylinder

unconventional geometry settings but may not be as suitable as analytical model that could study and give results for thousands of models during a parametric study or design optimization.

5. Parametric Study

The design parameters of the composite cylinder are further investigated to check their effect on the structure behavior under the same load and geometry. Using the previous example, the cylinder under consideration is consisted of 4 plies; all of which of the same material under internal pressure of 10 MPa with closed ends.

Starting with the winding angle as an important parameter in anisotropic material used in composite cylinders; a winding angle configuration $\pm\alpha$ with range of 0° to 90° degrees as a value of α in a four-ply cylinder is studied and the results given in figure 7 show the stresses and strains within the wall thickness of the cylinder.

A general note on all stresses and strains; at the start and end of the range of the winding angle (i.e. at $\pm 0^\circ$ and $\pm 90^\circ$) the results of all four plies have linear change in value without sudden or abrupt changes with ply migration within the thickness; this happens as the fibers tend to have the same direction which could mean that they may be considered as only one ply with the same winding angle. And to clarify that; at $\pm 0^\circ$ or $\pm 90^\circ$ the cylinder wall may be described as only one ply with 0° or 90° winding angle while at $\pm 30^\circ$ winding angle configuration; the cylinder wall may be described as $(+30^\circ/-30^\circ/+30^\circ/-30^\circ)$.

5.1. Analytical and finite element comparison

Figures (7-1) and (7-2) show the hoop stresses and strains respectively. As mentioned before the start and end of the winding angle show linear change in stresses and strains within the thickness which is quite convenient to use as sudden stress change tend to create inter-ply high shear values that could create structure instability and even delamination way before the material ultimate strength values leading to structure failure. As it appears from figure (8-1) some comfort zones for the winding angle choice are worth mentioning. The first is $(0^\circ-30^\circ)$ as the stress change is somehow smooth and without much difference between the stress at the inner and outer surface of the cylinder. The second is 90° as the stress is also linear and smooth but offers the highest stress difference between the inner and outer surface of the cylinder wall. The third is in the region around 68° as it may also offers somewhat smooth stress transition within thickness. Figure (8-2) is clear that more we get near the 90° winding angle, the less the strain within the wall thickness in the hoop direction meaning a stiffer structure, but it's also worth mentioning here that also around 68° winding angle is the local minimum of the strain's values even though it's not much different than 90° strain but it's an interesting phenomenon that may need further investigation to clarify.

5.2. Stresses and strains variation with winding angle

Figures (8-3) and (8-4) show the axial stresses and strains respectively. The comfort zones here are quite clear but by studying both figures simultaneously; the best of choice here would be $(0^\circ-10^\circ)$ and around 53° winding angles as they offer the least strains and the smoothest stresses. The $(0^\circ-10^\circ)$ range is quite clear to clarify as the axial stresses in those areas are mainly loaded on the fibers of the structure which has the stronger tensile stiffness strength. While the 53° range is explainable under the coupling between the pressure on the cylindrical wall and the closed ends and the usage of the netting analysis which could briefly described as the consideration of the cylinder as made of fibers only and the matrix strength is completely ignore and this angle offers the best resolution between hoop and axial stresses distribution according to pressurized cylindrical structure.

Figures (8-5) and (8-6) show the radial stresses and strains respectively. The strain figure offers the $(50^\circ\pm 3^\circ)$ range as the stiffest structure in the radial zone which could also be explained by the netting analysis as mentioned before. This could lead to that the netting analysis is worth considering greatly in the analysis of radial and axial stresses only which offer great agreement in the best winding angles range of $\pm 53^\circ$ configuration.

Figures (8-7) and (8-8) show the shear stresses and strains in the cylinder wall plane (Θ -z) direction respectively. Although these charts aren't quite cheerful in the point of smooth stress transition between plies but at least they offer a good insight into what to expect while choosing winding angles other than 0° and 90° , so that we could make sure the material and structure properties could with stand that kind of shear stresses values and transitions.

Figures (8-9) and (8-10) show the fiber and matrix tensile stresses respectively. And they may be considered a decision maker in the choice of winding angles configuration. It's well known that the tensile strength of fibers is much more of that of matrix strength, so it's only logical to choose the

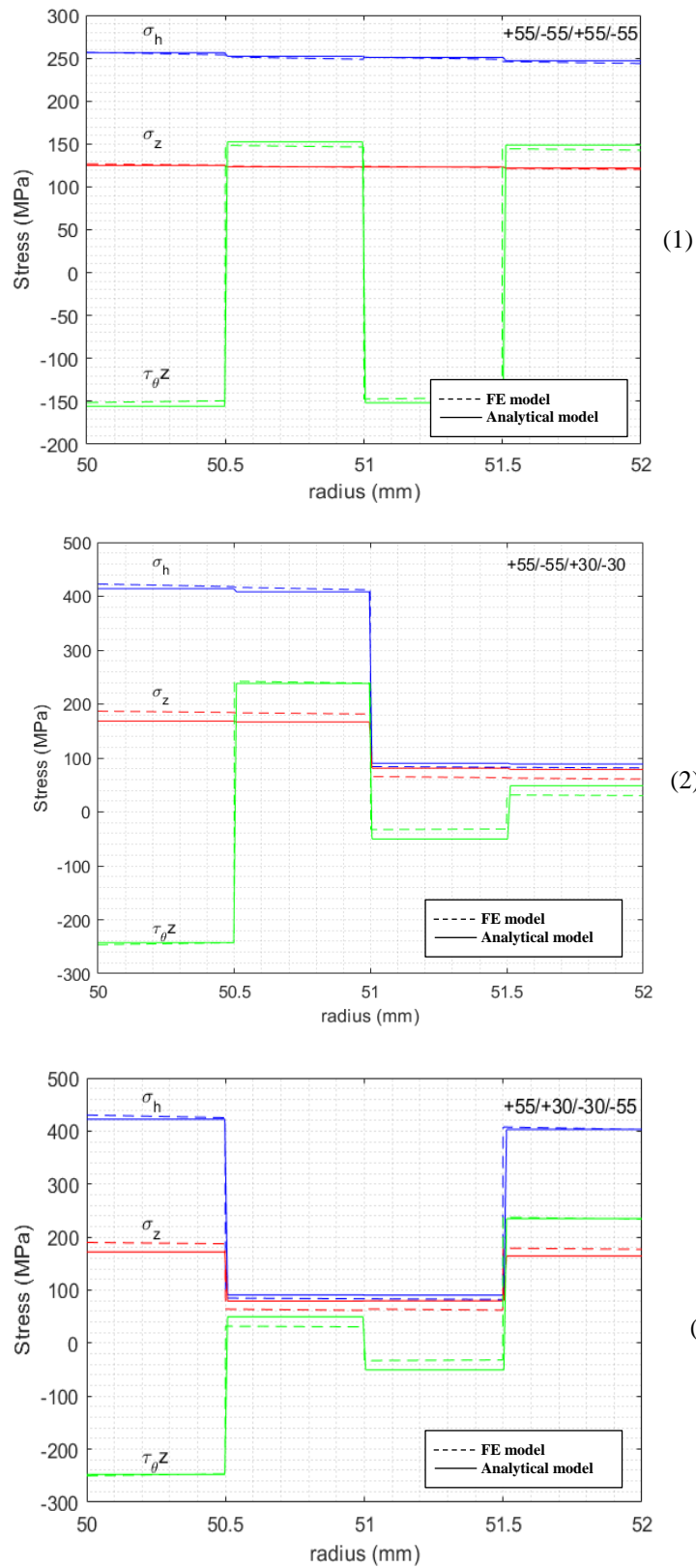
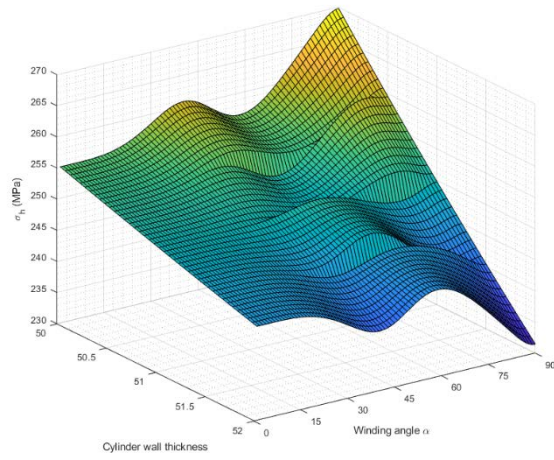
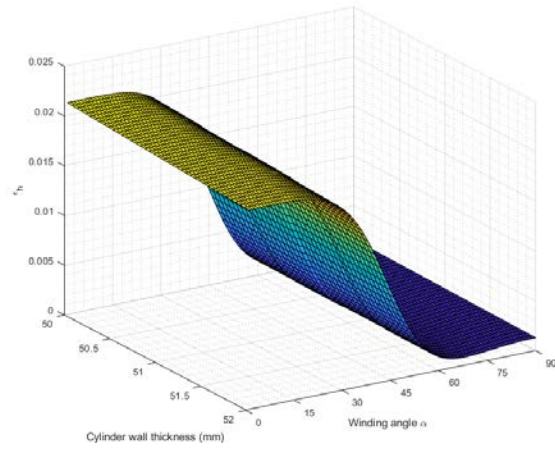


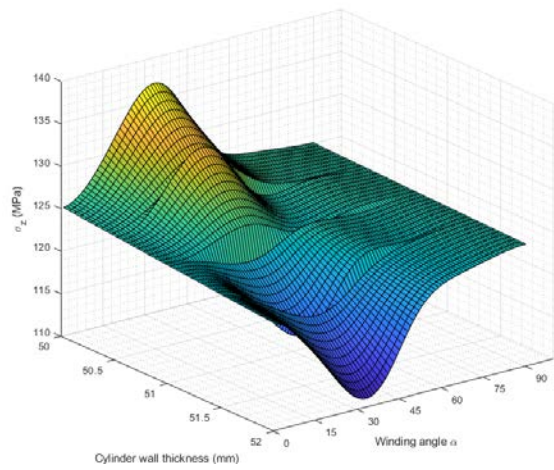
Figure 7. Stress distribution within thickness for a cylinder pressurized internally at 10 MPa using finite element analysis by ANSYS and analytical method for different stacking sequences



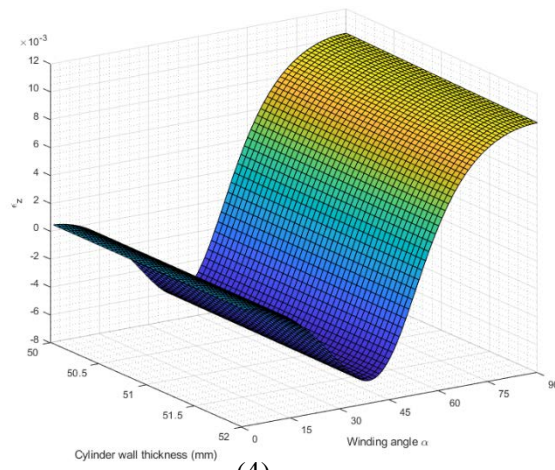
(1)



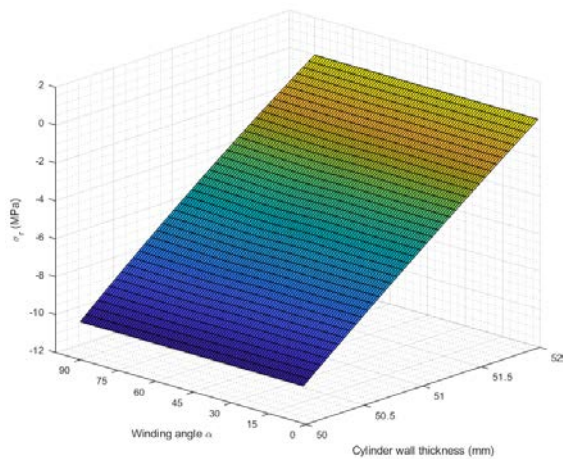
(2)



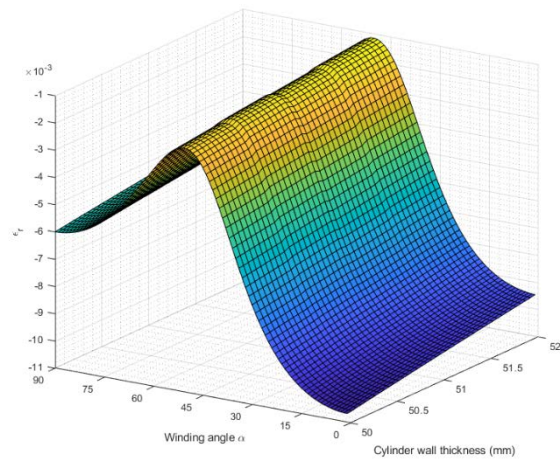
(3)



(4)



(5)



(6)

winding angle that offers the highest tensile stress on fibers and or the lowest tensile stress on matrix. And these two figures are actually complementary or very good to say that we could deduce one from

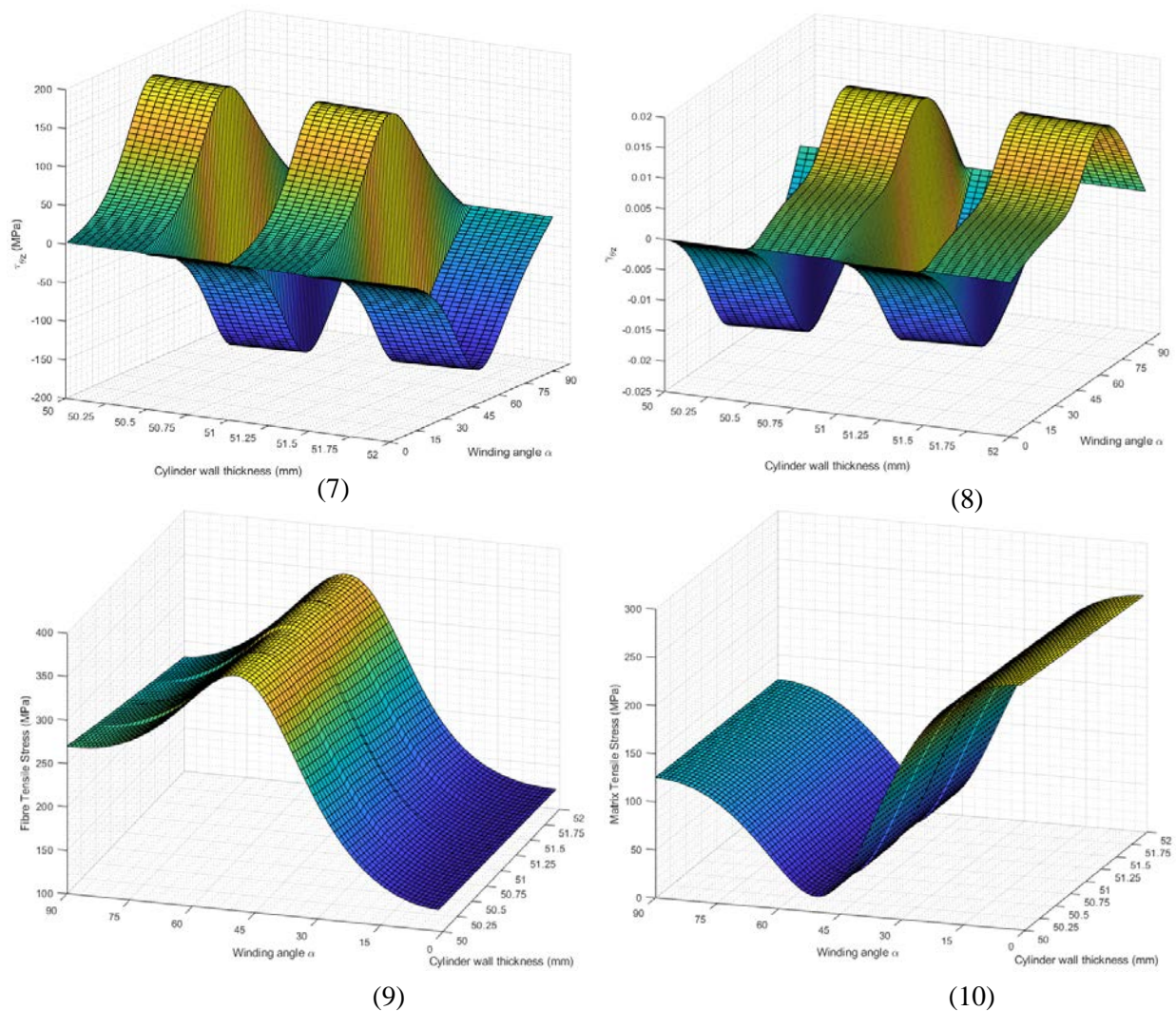


Figure 8. Stresses and strains distribution within the wall of Graphite-polymer composite cylinder (4plies) with closed ends pressurized internally under 10 MPa with winding angles $\pm\alpha$ configuration

the other as the tensile stress is loaded one or both of them. The figures offer the $(51^\circ \pm 3^\circ)$ as the best choice to load most of the tensile stresses on the fibers as they have the best strength in the structure.

Although 3 cases are being investigated in the previous section; FEA is somehow time and resource consuming in the preliminary design phase where a parametric study of many inputs need to be studied to check the impact of every composite parameter for sensitivity of the final product to that parameter. Stacking sequence can vary a lot and is proven to be very effective in the safety of the final product; an optimization or a further investigation of many cases should be performed specially in the products with complex loading conditions (biaxial or triaxial loads) as these cases can require hundreds of checkups and geometry variations that can't be done efficiently on FEA or as easy as on mathematical modeling.

5.3. Ply thickness effect on stresses variation

Also, one of the affecting design parameters is the thickness of the single ply, figure 8 shows when increasing the number of plies within the same thickness, i.e. winding the same angle many times over until reaching specific thickness then changing the angle to the negative value, to study the effect of varying the winding angle over and over again until reaching the required thickness or is it better to stay on the same angle until a specific thickness and then change the angle. And the figure shows that staying on the same angle for large thickness without varying the angle periodically may create some kind of stress instability and larger maximum stresses in the overall thickness as the large variation between the maximum and the minimum value of the interlaminar stresses may create some kind of internal stresses that could lead to severe delamination. It is notable to say that the ability to increase the thickness may be only available via automated fibre placement method of winding as the conventional filament

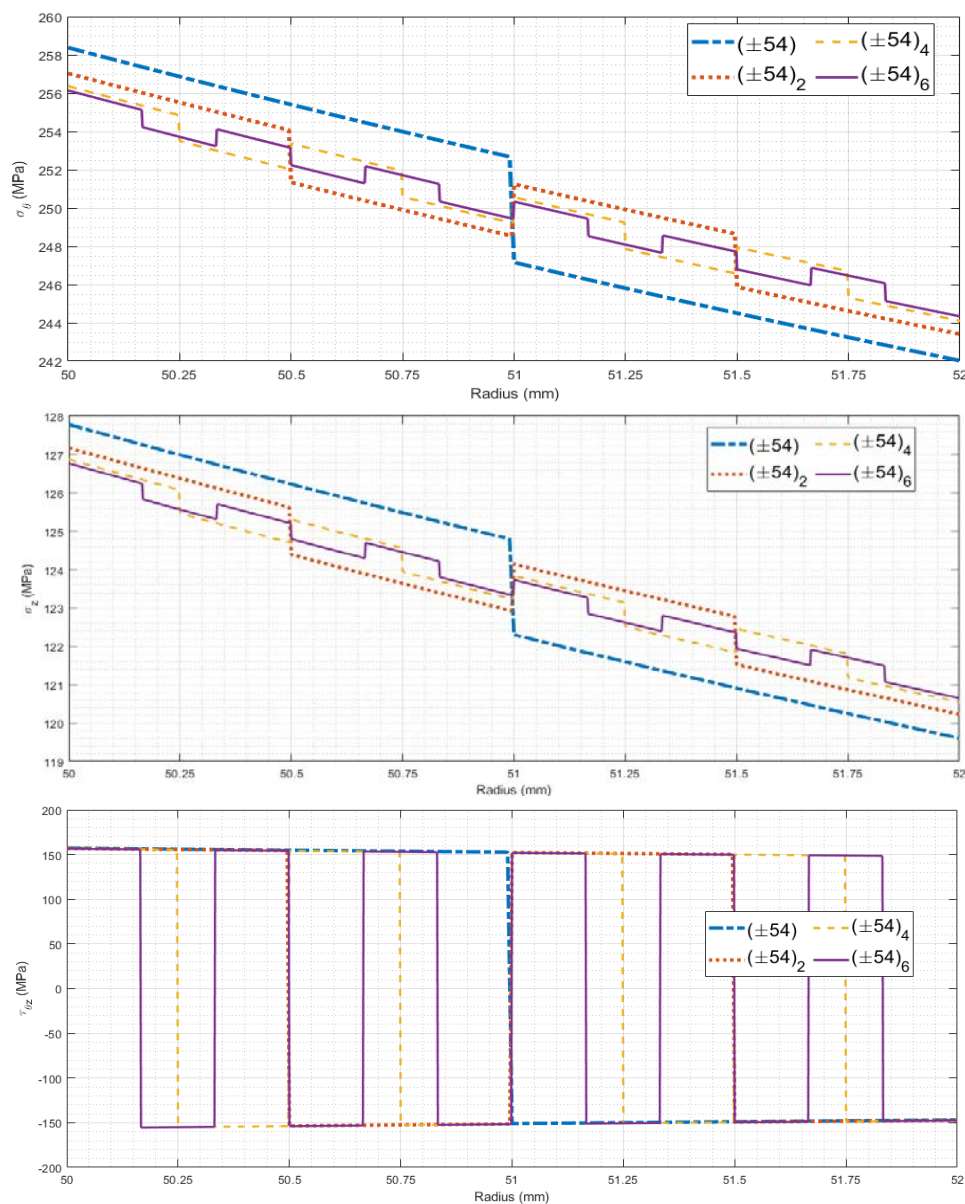


Figure 9. Stress distribution in UD Kevlar cylinder wall under internal pressure of 10 MPa for different ply thickness configurations

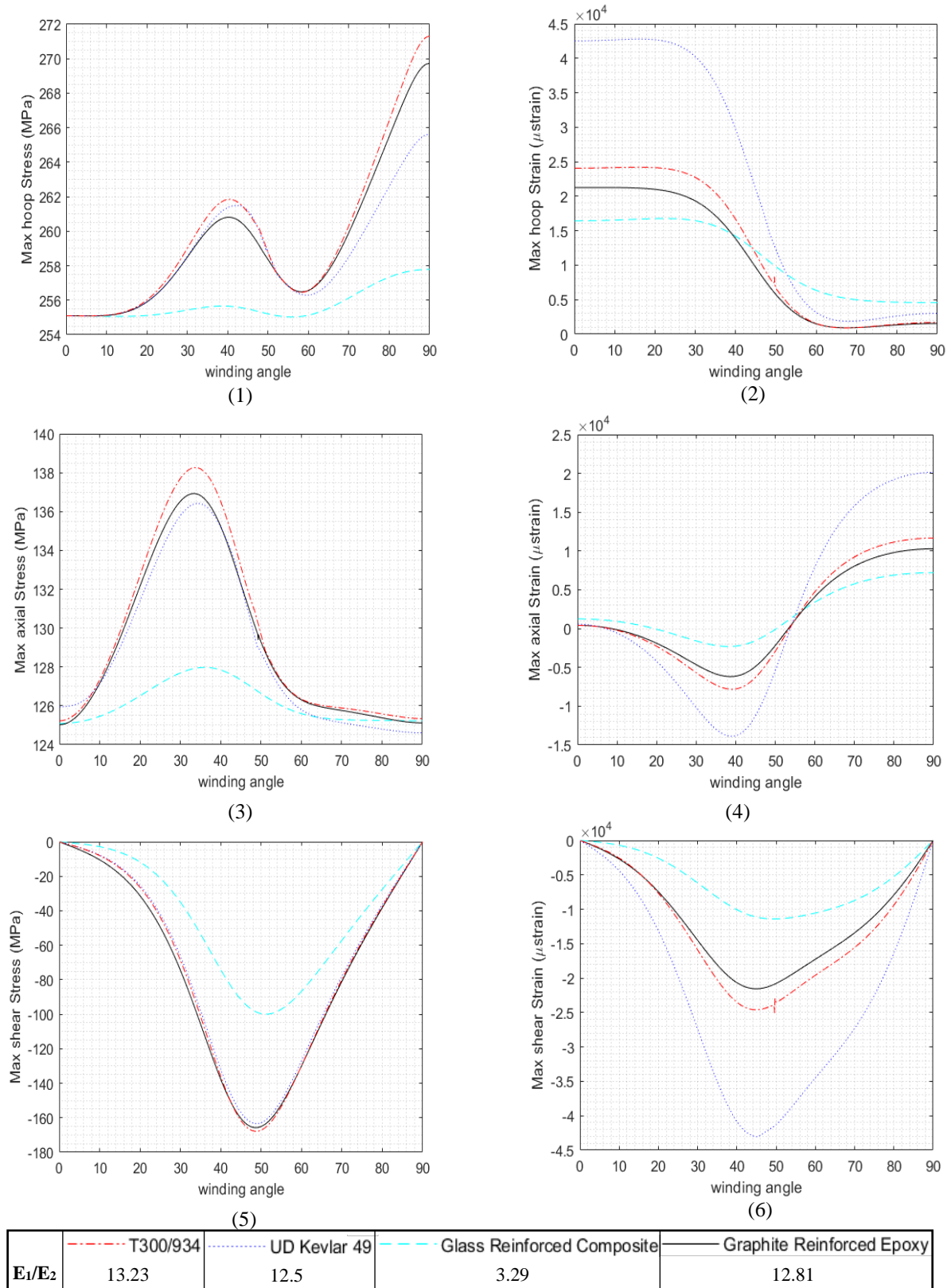


Figure 10. Absolute maximum values of stresses and strains within wall thickness of different materials composite cylinder (4 plies) with winding angles $\pm\alpha$ configuration

winding machine could only achieve reciprocating winding angle between positive and negative values of the defined winding angle by the designer.

5.4. Different material effect on stress variation

Figure (10) shows maximum absolute values of stresses and strains for different materials with different winding angles. Starting with 0° winding angle where the fiber is placed along the z-axis this angle is considered the worst choice for pressure vessels under internal pressure only as in this angle the resistant to the pressure is the matrix tensile strength which is the worst in comparable with the fiber strength.

Figure 10 shows the stresses and strains maximum values for different winding angles (0° - 90°) for a cylinder of 4 plies with internal radius of 50 mm and thickness of 2 mm for all plies. As shown from figure 8 stresses vary along the thickness and the maximum stress within the thickness is chosen as a representing value for each winding angle for these charts. An internal pressure of 10 MPa load and normal forces due to closed ends on the cylinder ends are the principal loads on the charted cylinder. The stacking sequence is $\pm\alpha$ for all plies starting from the inside ply.

Figures 10.1, 10.2 show the maximum hoop stresses and strains within the thickness of the cylinder wall for all winding angles in a stacking sequence of $\pm\alpha$. Although the stresses appear to be at a minimum value at near zero angles but if we look at the strain values at the same periods, we'll see that it has the maximum value which is logical as the winding angle zero means all the fibers are axial to the cylinder and the only resistance to the pressure load is the matrix tensile strength which has much lower modulus and strength. In terms of hoop strain the best choice for the winding angle would be angles more 45-50 degrees and up to 90 degrees, but the best choice according to the study for this case would be more than 60 degrees and for some materials as carbon fibers (T300 and Graphite) would be around 65 degrees as it presents the lowest hoop strains. In combination with stresses chart the best choices for winding angles would be less than 20 degrees and the period of 55-60 degrees; in which the first choice would be unacceptable due to large strains so the logical choice would be the latter.

Figures 10.3, 10.4 showing the axial stresses and strains offer us the green zones for choosing the winding angles at less than 10 degrees and more than 55 degrees for the stresses. While for strains the best choices would be less than 20 degrees and somewhere between 45-60 degrees. So, in terms of axial stresses and strains the best choice for winding angle would be either less than 10 degrees or 55-60 degrees.

Figures 10.5, 10.6 charting the shear stresses and strains offers the best winding angles at less than 20 degrees and more than 80 degrees for the stresses, and almost the same periods for the strains.

In general, the used mathematical model can be tailored to produce any required stresses or strains within the thickness of a composite laminated cylinder to use these results to investigate the impact of changing any one the production parameter or check the safety of the composite cylinder as explained in the next section.

6. Failure Criteria

Composite use many failure theories that can be compared with the output stresses of the analysis giving a safety factor or usability to the structure. In the following part a couple of the most commonly used composite failure will be demonstrated using the stress analysis results from the mathematical model.

6.1. Tsai Wu

$$F_1\sigma_1 + F_2\sigma_2 + F_{11}\sigma_1^2 + F_{22}\sigma_2^2 + F_{66}\tau_{12}^2 - \sqrt{F_{11}F_{22}}\sigma_1\sigma_2 \leq 1 \quad (29)$$

Where

$$F_1 = \left(\frac{1}{s_1^T} + \frac{1}{s_1^C}\right), \quad F_{11} = -\frac{1}{s_1^T s_1^C}, \quad F_2 = \left(\frac{1}{s_2^T} + \frac{1}{s_2^C}\right), \quad F_{22} = -\frac{1}{s_2^T s_2^C}, \\ F_{66} = \left(\frac{1}{s_{12}^F}\right)^2$$

Such that [15]:

- σ_i is normal or transverse stress according to the subscript (σ_1 is stress along the fiber direction and σ_2 is stress transverse to the fiber direction)
- S_j^i is the strength (i for compression or tension strength, j for direction of strength load)

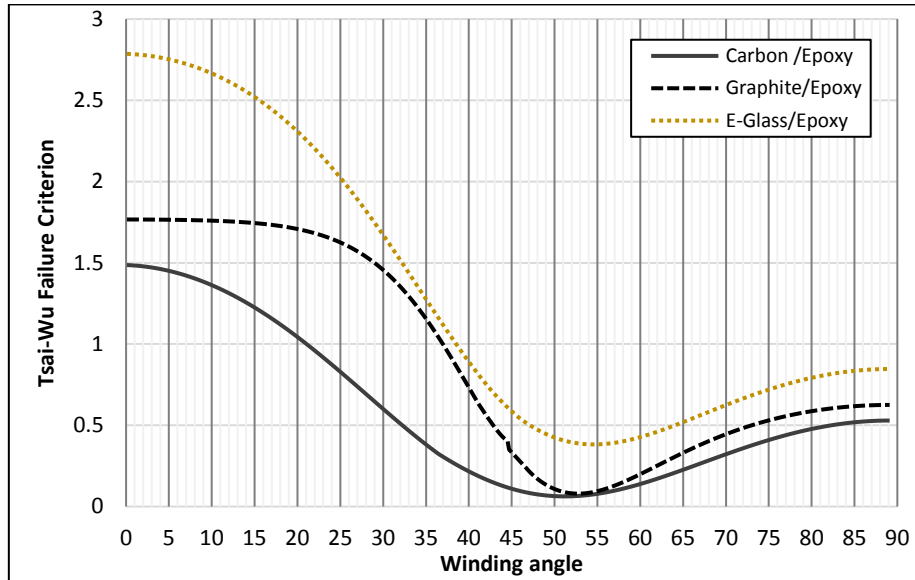


Figure 11. Tsai-Wu safety criterion variation with winding angle

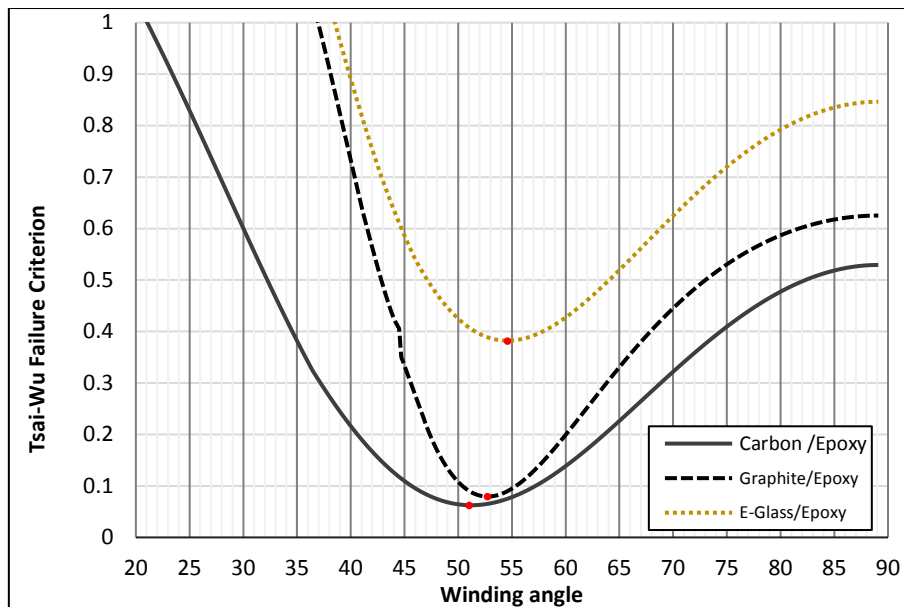


Figure 12. Winding angle safe zone (zoomed of figure 11)

Figures 11-12 show a cylinder of 50mm radius, thickness 4 mm manufactured with 4 plies of stacking ($\pm\alpha$) and internal pressure of 5MPa and closed ends (biaxial load); with the variation of the winding angle to check the first ply failure using the Tsai-Wu failure criterion figure 12 shows the safe zone of winding angle choice which varies according to the material type due to variation of strength and anisotropic ratio. The analysis shows that for carbon / epoxy the winding angle could be chosen between 21° and 90° with the safest choice around 51°, while for E-glass / epoxy the safe winding choice starts

at 39° and the safest choice is around 54°. This change in optimum angle could be explained as the strength of the material increases the winding angle safe zone widens and the safest choice is dependable on the anisotropic nature of the material.

6.2. Tsai Hill

Based on the energy theory the Tsai-Hill criterion is

$$\left(\frac{\sigma_1}{S_1}\right)^2 - \left(\frac{\sigma_1\sigma_2}{S_1^2}\right) + \left(\frac{\sigma_2}{S_2}\right)^2 + \left(\frac{\tau_{12}}{S_{12}}\right)^2 \leq 1 \quad (30)$$

Analogous to the Von-mises criterion the Tsai-Hill failure criterion is considered one of the most used for orthotropic material as a failure criteria for design calculations [18].

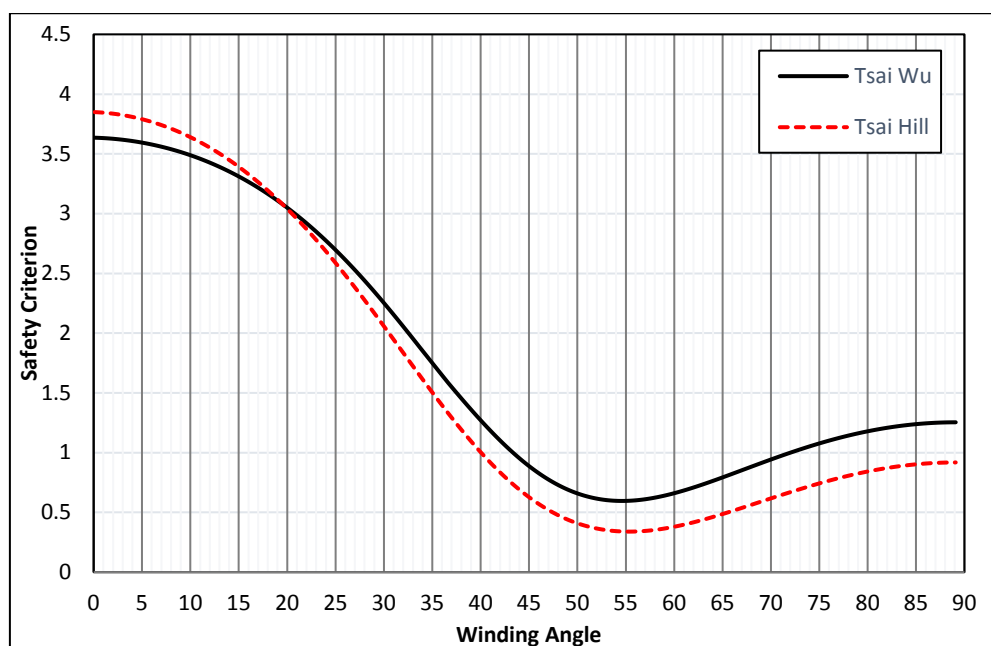


Figure 13. Comparison between Tsai-Wu and Tsai-Hill failure criteria and winding angle

Figure 13 shows that Tsai-Wu criterion is more conservative than Tsai-Hill in the safest winding angle zone as it gives less safe criterion number. An application of different failure criteria is beneficial to decrease the number of experiments required to test the final product or application.

Table 3. Optimum winding angles according to failure criteria

Optimum winding angle	Carbon / Epoxy $E_1/E_2=14.27$	Graphite / Epoxy $E_1/E_2=12.81$	E-Glass / Epoxy $E_1/E_2=3.94$
Netting Theory	54.74 °		
Tsai Wu	51.3 °	52.8 °	54.6 °
Tsai Hill	53.3 °	54.4 °	55.3 °

Table 3. shows the optimum winding angle according to different failure theories and from the output of the stress analysis by applying each stress value and comparing it to the material strengths. This shows us that according to the material properties and different loading conditions, the winding angle with the least chance to fail could change slightly or greatly, i.e. for custom material the material properties anisotropic factor E_1/E_2 could vary largely affecting the optimum winding greatly. As netting theory mainly depends on the existence of fibers only in the analysis only a single optimum winding angle is

provided for the same loading condition (for a pressure vessel with closed ends that optimum angle is 57.74°) no matter what the material properties or its anisotropic nature.

7. Conclusion

Lekhnitskii's formalism [1] is modified to incorporate the internal and external pressure loading beside the axial, torsional and bending loads for multilayered composite cylinder.

A numerical example for a composite cylinder subjected to internal pressure and axial tension is presented and the resulted stresses and strains within wall thickness are illustrated. These results are used to validate a built-up finite element model; the results are found to be comparable from both the analytical and the finite element model.

The modified analytical model is used to perform a parametric study for a composite cylinder subjected to internal pressure and axial tension, the results show the effectiveness of material anisotropy such that the higher E_1/E_2 the higher the variation of stresses with the winding angle.

Also, from the parametric study, one could conclude that the layer thickness is an effective parameter; as the layer thickness decreases, the obtained stresses through wall thickness is found to be smoother and have lower value.

The output of the stress analysis can be used in the safety check using any safety criteria, they are key to the design and geometry to perform such analysis is the design phase. The results of the safety criteria show that using the winding angle between $50-55$ is the safest choice for biaxial load of pressure vessels and this agrees with the netting analysis with mild variation due to the matrix factor in strengthening the final product.

References

- [1] S. G. Lekhnitskii, *Theory of elasticity of an anisotropic elastic body*. Holden-day, 1963.
- [2] S. C. Panda and R. Natarajan, "Finite element analysis of laminated composite plates," *International Journal for Numerical Methods in Engineering*, vol. 14, no. 1, pp. 69-79, 1979.
- [3] S. Panda and R. Natarajan, "Analysis of laminated composite shell structures by finite element method," *Computers & Structures*, vol. 14, no. 3-4, pp. 225-230, 1981.
- [4] C. Jolicœur and A. Cardou, "Analytical solution for bending of coaxial orthotropic cylinders," *Journal of engineering mechanics*, vol. 120, no. 12, pp. 2556-2574, 1994.
- [5] P. Wild and G. Vickers, "Analysis of filament-wound cylindrical shells under combined centrifugal, pressure and axial loading," *Composites Part A: Applied Science and Manufacturing*, vol. 28, no. 1, pp. 47-55, 1997.
- [6] H. Bakaiyan, H. Hosseini, and E. Ameri, "Analysis of multi-layered filament-wound composite pipes under combined internal pressure and thermomechanical loading with thermal variations," *Composite Structures*, vol. 88, no. 4, pp. 532-541, 2009.
- [7] X. Sun, V. Tan, Y. Chen, L. Tan, R. Jaiman, and T. Tay, "Stress analysis of multi-layered hollow anisotropic composite cylindrical structures using the homogenization method," *Acta Mechanica*, vol. 225, no. 6, pp. 1649-1672, 2014.
- [8] M. Menshykova and I. Guz, "Stress analysis of layered thick-walled composite pipes subjected to bending loading," *International Journal of Mechanical Sciences*, vol. 88, pp. 289-299, 2014.
- [9] D.-C. Pham, N. Sridhar, X. Qian, A. J. Sobey, M. Achintha, and A. Shenoi, "A review on design, manufacture and mechanics of composite risers," *Ocean Engineering*, vol. 112, pp. 82-96, 2016.
- [10] I. A. Guz, M. Menshykova, and J. K. Paik, "Thick-walled composite tubes for offshore applications: an example of stress and failure analysis for filament-wound multi-layered pipes," *Ships and Offshore Structures*, vol. 12, no. 3, pp. 304-322, 2017.
- [11] V. Mohanavel, S. Prasath, M. Arunkumar, G. Pradeep, and S. S. Babu, "Modeling and stress analysis of aluminium alloy based composite pressure vessel through ANSYS software,"

Materials Today: Proceedings, 2020.

- [12] P. Sharma et al., "Theoretical analysis of design of filament wound type 3 composite cylinder for the storage of compressed hydrogen gas," *International Journal of Hydrogen Energy*, vol. 45, no. 46, pp. 25386-25397, 2020.
- [13] S. K. Moshir, S. V. Hoa, F. Shadmehri, D. Rosca, and A. Ahmed, "Mechanical behavior of thick composite tubes under four-point bending," *Composite Structures*, vol. 242, p. 112097, 2020.
- [14] M. Xia, H. Takayanagi, and K. Kemmochi, "Analysis of multi-layered filament-wound composite pipes under internal pressure," *Composite structures*, vol. 53, no. 4, pp. 483-491, 2001.
- [15] M. W. Hyer and S. R. White, *Stress analysis of fiber-reinforced composite materials*. DEStech Publications, Inc, 2009.
- [16] M. Jones, "The basic ply properties of a Kevlar 49/epoxy resin composite system," *Royal Armament Research And Development Establishment Fort Halstead (England)*, 1983.
- [17] I. M. Daniel, O. Ishai, I. M. Daniel, and I. Daniel, *Engineering mechanics of composite materials*. Oxford university press New York, 2006.
- [18] D. Gay, *Composite materials: design and applications*. CRC press, 2014.